SCIENTIFIC REPORTS

OPEN

SUBJECT AREAS:
MATERIALS FOR OPTICS
SEMICONDUCTORS
POLARITONS
OPTICS AND PHOTONICS

Received
14 October 2013

Accepted
29 November 2013

Published
19 December 2013

Correspondence and requests for materials should be addressed to H.L. (liheng3000@xmu.edu.cn) or J.Y.K. (jykang@xmu.edu.cn)

Vacuum Rabi Splitting of Exciton–Polariton Emission in an AlN Film

Kongyi Li[1], Weiying Wang[2], Zhanghai Chen[3], Na Gao[1], Weihuang Yang[1], Wei Li[2], Hangyang Chen[1], Shuping Li[1], Heng Li[1], Peng Jin[2] & Junyong Kang[1]

[1]Funjian Key Laboratory of Semiconductor Materials and Applications, Department of Physics, Xiamen University, Xiamen 361005, China, [2]Key Laboratory of Semiconductor Materials Science and Beijing Key Laboratory of Low–dimensional Semiconductor Materials and Devices, Institute of Semiconductors, Chinese Academy of Sciences, Beijing 100083, China, [3]State Key Laboratory of Surface Physics, Key Laboratory of Micro and Nano Photonic Structures (Ministry of Education), Department of Physics, Fudan University, Shanghai 200433, China.

The vacuum Rabi splitting of exciton–polariton emission is observed in cathodoluminescence (CL) and photoluminescence spectra of an AlN epitaxial film. Atomic force microscopy and CL measurements show that the film has an atomically flat surface, high purity, and high crystal quality. By changing the temperature, anticrossing behavior between the upper and lower polariton branch can be obtained in low temperature with a Rabi splitting of 44 meV, in agreement with the calculation. This large energy splitting is caused by strong oscillator strength, intrinsically pure polarization in wurtzite AlN semiconductor, and high fraction of free exciton in the sample. These properties indicate that AlN can be a potential semiconductor for the further development of polariton physics and polariton–based novel devices.

In the past three decades, the exciton–polariton in semiconductors has attracted considerable attention in both practical and theoretical research because of its strong light–matter coupling, bosonic effects, and various interesting properties in terms of quantum optics and spin–optoelectronic. Currently, numerous experiments have focused on observing the coherence effects of exciton–polariton at low temperature, including phase transition, superfluidity, superradiance, and entanglement. With the assistance of microcavity structure and the rapid development of crystal growth technology, the emphasis of study on exciton–polariton coherence is on higher operating temperature or lower critical density for the Bose–Einstein condensation[1,2] and spontaneous emission, parametric amplification, and spin–memory of polariton–based novel devices, among others[3–5]. Given its prefect crystal quality, GaAs– or CdTe–based structures first achieved exciton–polariton coherence at cryogenic temperature. However, the exciton–polariton in those semiconductors suffers from weak exciton oscillator strength, small exciton binding energy, and small longitudinal–transverse (L–T) splitting energy. Moreover, low phonon energy and phonon scattering rate at liquid helium temperature, for example in GaAs, may result in a lower branch bottleneck, i.e., a large depletion at the bottom region relative to high k states, which remarkably limits the emission from coherent condensate state[6]. Recently, numerous studies have focused on the wide bandgap semiconductors ZnO[7,8] and GaN[9] because of their large binding energies (60 meV for ZnO and 25 meV for GaN), which can survive at room temperature. The oscillator strengths of ZnO and GaN are approximately one order of magnitude larger than that of GaAs[10].

In the AlN semiconductor, the binding energy of free exciton can reach up to 55 meV[11], which is higher than that of GaN and close to that of ZnO. The 7.3 meV splitting energy between the longitudinal and transverse exciton mode of AlN is almost seven times larger than the splitting in GaN[12]. Having the largest direct bandgap (~6.2 eV) among available semiconductors, AlN is a potential semiconductor in deep–ultraviolet solid–state light source. In contrast to ZnO–based devices limited by *p*–type doping, AlN has already been fabricated into *p*–*i*–*n* homo–junction light–emitting diode (LED) with electroluminescence peak at 210 nm at room temperature[13,14]. Therefore, AlN can be considered as the future light source of quantum information processing because of its high channel capacity in communication. Recently, the epitaxy technique of AlN semiconductor has undergone major developments, leading to a dramatic improvement of crystal quality[11,15]. However, no direct evidence or striking spectral indication of exciton–polariton emission has been obtained in AlN, which can be attributed to the lack of high quality and high purity samples.

To explore the fundamental physics and potential applications of exciton–polariton in a new system, we are working on the preparation of AlN high quality and purity epitaxial films via metalorganic vapor phase epitaxy

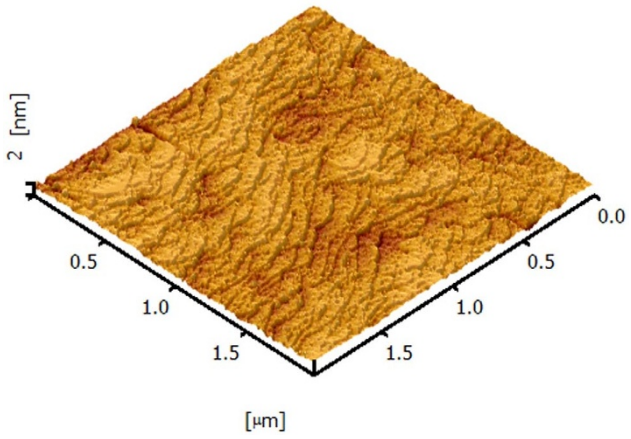

Figure 1 | AFM image (2 μm × 2 μm) of an AlN epilayer, in which atomic steps can be observed.

(MOVPE). Optical properties can be characterized through temperature–dependent cathodoluminescence (CL) and photoluminescence (PL) measurements, thereby allowing us to reveal more exciton behavior and interactions in AlN under different temperatures.

Results

Under atomic force microscopy (AFM), the morphology of the AlN sample exhibits an atomically flat surface (RMS = 0.16 nm) with atomic steps (Figure 1), which reveal good quality with layer–by–layer growth. Figure 2(a) shows the CL spectrum of the AlN epilayer measured at 80 K. The spectrum is dominated by the line at 6.030 eV. Three additional distinct peaks with similar line shapes but weaker intensities are resolved at low energy side. To examine the origin of luminescence peaks, CL spectra were measured with temperature increasing. Energy separations between the main line at 6.030 eV to each emission peak are plotted in Figure 2(b). As the temperature increases, these peaks follow the dominated line with almost the same energy interval, thus revealing that the peaks have similar origins. Given that the energy interval 106 meV is approximately equated to the longitudinal optical (LO) phonon energy[16], we assign three distinct peaks as the LO phonon–assisted emissions of the dominated line. Considering the energy position of 6.030 eV at 80 K and its visibility up to 265 K, the dominated line is identified as free A–exciton related transition, which agrees with Ref. 11. A shoulder at 6.080 eV, which is higher than the main line, is noted. Similarly, a small shoulder with similar energy interval can be observed on the right side of each LO replica. Thus, we consider that the small shoulders originated from the same physical mechanism as that of the LO phonon–assisted emission. Generally, luminescence peak with energy higher than that of the free A–exciton can be associated to the excited state (n = 2) or B– and C–exciton (crystal–field splitting). However, the energy spacing of 50 meV in our CL spectra is higher than the reported values between the ground state and the excited state (approximately 40 meV[11,17–19]) and lower than the predicted energy of the crystal–field splitting (more than 100 meV[20]). Compared with the measurements of other groups at the same temperature region[11,15], no obvious luminescence peak related to bound–exciton recombination is visible in the CL spectra. Nevertheless, up to three–order LO phonon replicas are observed. These findings verify the high purity and crystal quality of the sample. Crystal with high purity and quality will result in high fraction of free exciton and coupling of free exciton and photon and then to form exciton–polariton. These quasi–particles typically have an anticrossing behavior in dispersion relation. To clarify the origin of this shoulder at 6.080 eV, we extend temperature to liquid helium.

Similar to the above CL studies, PL spectrum at 5.8 K is dominated by free A–exciton related emission at 6.023 eV, as shown in Figure 3. At its high–energy side, the shoulder we focus on can be distinguished well at 6.078 eV. The entire luminescence spectrum shifts as a function of temperature, except for the peak labeled "S" at 6.139 eV. This peak is assigned as an unintentional Raman scattering line from the copper sample stage because this line still existed when the sample was discarded. Unlike the typical temperature–dependent variation of bandedge emission, the energies of both the main line and its higher energy shoulder do not show monotonous shifting with temperature decreasing (see Figure 3). At high temperature region, the main line shifts toward higher energy, as expected. However, when the temperature drops to lower than 60 K, the redshift is observed. Considering the main line keeps a similar line shape with linewidth of around 20 meV, this redshift cannot be explained by an evolution from free exciton recombination toward neutral donor bound recombination. When temperature is below 100 K, the higher energy shoulder can be distinguished from the "S" peak. It keeps a redshift with temperature decreasing, but stays at the energy of 6.078 eV after 20 K. These special behaviors differ from the spectral shift of exciton with temperature.

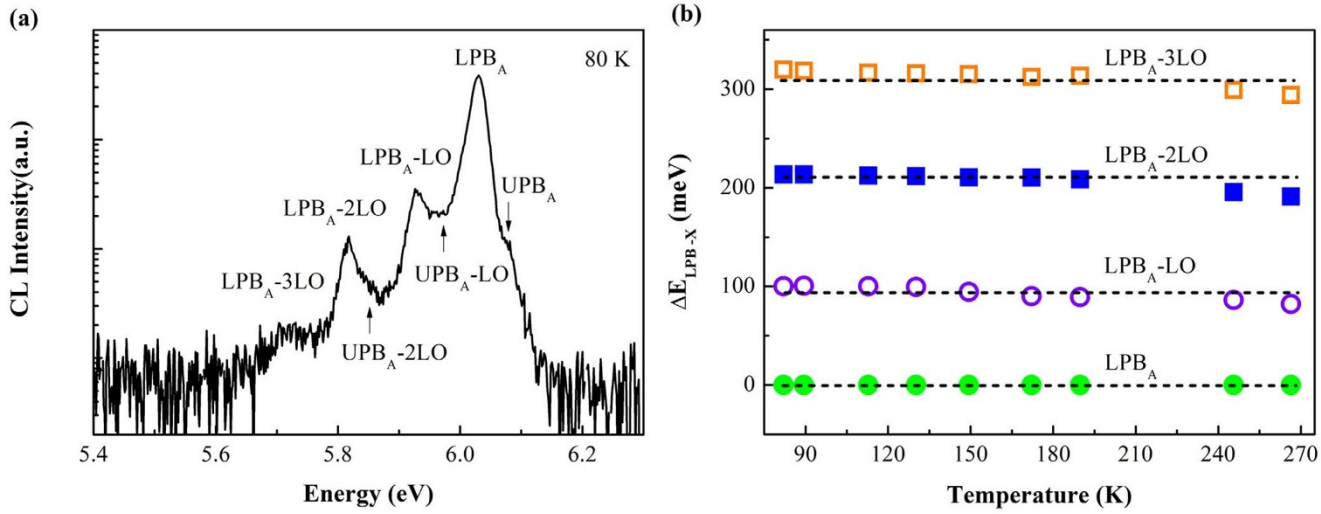

Figure 2 | Temperature–dependent CL measurements. (a), CL spectra of an AlN film measured at 80 K. (b), Temperature evolution of energy separations between the LPB_A and each luminescence line from 265 K to 80 K, exhibiting almost the same trends with LPB_A shifting. The dash lines are guides for eyes.

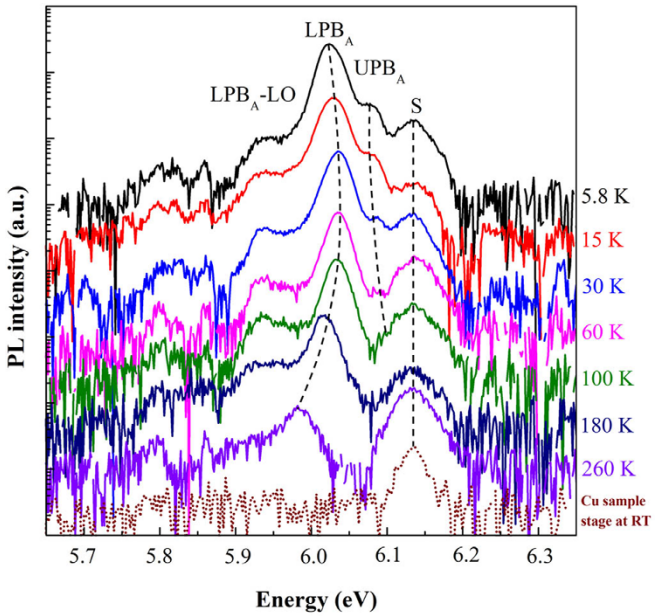

Figure 3 | Temperature–dependent PL taken in temperatures ranging from 260 K to 5.8 K. The dash lines are guides for viewers. The "S" peak represents the unintentional Raman scattering line from the sample stage. The dot line below shows the spectrum of copper sample stage at room temperature (RT).

In the case of several exciton states, the energy versus wavevector polariton dispersion can be described by the dielectric approximation as following equation[21],

$$\frac{\hbar^2 c^2 k^2}{E^2} = \varepsilon_b + \sum\nolimits_i \frac{F_i E_{Ti}^2}{E_{Ti}^2 - E^2 + \beta_i k^2 - iE\gamma_i}, \qquad (1)$$

where ε_b is the background dielectric constant, $\beta_i = E_{Ti}/M_i$, E_{Ti} and M_i are the transverse exciton energy and the effective exciton mass respectively, γ_i is the exciton damping constant and F_i is the oscillator strength. Considering a large energy interval between A– and B–exciton and dipole–active states allowed for $\boldsymbol{E}\|c$ polarized light, here we only consider single excitonic resonance (A–exciton), i.e. $i = 1$. Given that E_T follows the temperature dependence of bandgap and dielectric constant (or refractive index) also changes with temperature, the anticrossing characteristics of exciton–polariton can be exhibited by temperature variation[4]. The temperature dependence of bandgap can be described by the Varshni model of $E(T) = E(0) - \alpha T^2/(\beta + T)$ with $\alpha = 1.8$ meV/K and $\beta = 1462$ K, and the Bose–Einstein model of $E(T) = E(0) - 2a_B/[exp(\Phi_B/T) - 1]$ with $a_B = 471$ meV/K and $\Phi_B = 725$ K for AlN semiconductor[22]. The dielectric constant, generally, varies linearly with temperature, and can be simply described by an empirical formula: $\varepsilon(T) = \varepsilon(0)(1 + \lambda T)$, where $\varepsilon(0)$ is the dielectric constant at 0 K and $\lambda(\equiv \varepsilon(0)^{-1}d\varepsilon/dT)$ is the temperature coefficient. Typically λ is of the order of 10^{-4} per K[23], so that the change of ε_b with temperature is much weaker than that of E_T. Differed from in cavity structure, light emission in an AlN film cannot achieve a pure geometry ($\boldsymbol{k} \perp c$) and polarization ($\boldsymbol{E}\|c$). The oscillator strength F_i of 1.14×10^{-2} for AlN[12] should be corrected with a factor $sin^2\Theta$[24], in which the Θ is the angle between a vector parallel to the c–axis and the wave vector $\boldsymbol{k}$ of photon (see Figure 4(a)). The damping factor γ_i is about $0.5\Delta_{LT}$[21], $\Delta_{LT} = \hbar\omega_L - \hbar\omega_T$. By using the characteristic parameters above, the exciton–polariton dispersions of AlN at different temperatures are calculated. As shown in Figure 4(b), the entire dispersion curve shifts to high–energy region with temperature decreasing. The bottleneck region, from where light is usually emitted, is located around 45°. In our experiment, the collection angle θ is also fixed at 45°. The energy of polariton from corresponding $\boldsymbol{k}$–state with temperature variation, thereby, can be calculated from this angle.

Figure 5(a) gives the energy variation of the main line in PL spectra from 5.8 K to 300 K. The calculated curve (solid line) reproduces the peak shifting very well over the entire temperature region, in particular, the redshift deviated from an exciton behavior (Varshni model) at lower temperature region. Furthermore, we calculated the curves for both LPB_A and UPB_A at lower temperature region, shown in Figure 5(b), which is also consistent with the experimental energy variations of the main line and its higher energy shoulder in PL and CL. The insert figure gives the calculated energy splitting between upper and lower branch as the function of temperature. The splitting energy reaches the minimum of 46.7 meV at 17 K, close to the value of 44 meV obtained from PL measurement at 20 K. This

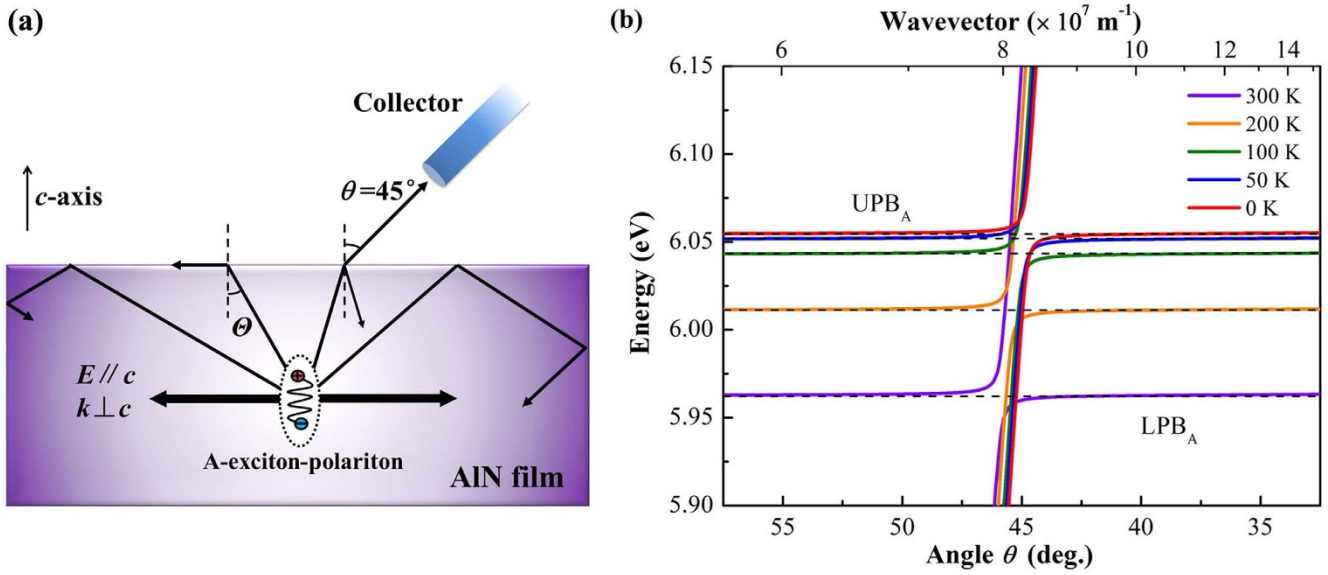

Figure 4 | Schematic diagram of experimental geometry of optical measurement and calculated temperature dependent exciton–plariton dispersion relation. (a), The collection angle θ is fixed at 45°, and Θ is defined as the angle of total reflection. The polariton emission of A–exciton is strongly polarized in the geometry of $\boldsymbol{E}\|c$ and $k \perp c$, most of which is confined by total internal reflection as in a natural resonator. (b), Calculated temperature dependent exciton–plariton dispersion relation for A–exciton of AlN. Dash lines represent the unperturbed exciton branches at different temperatures.

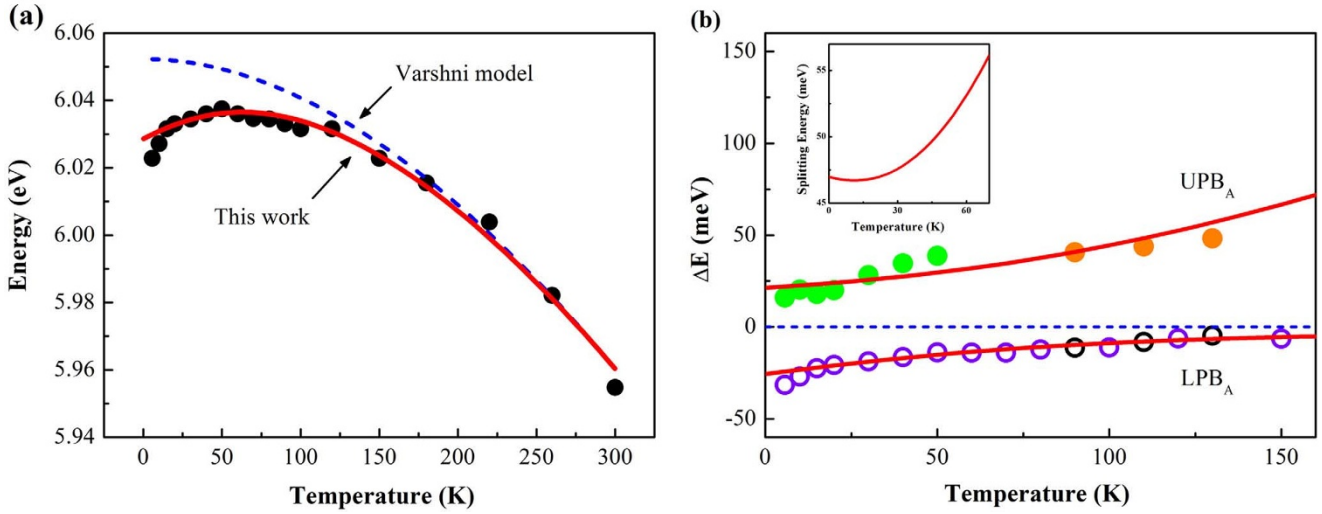

Figure 5 | Variation of polariton energy position as a function of temperature. (a), Solid dots show the variation of lower polariton energy with temperature in PL measurement. The dash and solid line indicate the calculated results from the Varshni model and our numerical simulation, respectively. (b), The energy separation between the upper and lower polariton branches acts as the function of temperature by discarding the component of band–edge shifting using Varshni model which show as the dash line. The violet open circles and green solid circles are extracted from PL measurement. The black open circles and orange solid circles are from CL measurement. Solid curves are the result of numerical simulation and the insert gives the corresponding splitting energy varied with temperature.

anticrossing behavior confirms a strong light–matter coupling regime, namely, an exciton–polariton formation in sample. On the basis of analysis above, we assign the dominated line at 6.023 eV as the lower polariton branch of A–exciton (LPB_A) and the higher energy shoulder at 6.078 eV as the upper polariton branch (UPB_A).

In semiconductor, the light propagating in crystal usually couples to the transverse mode of exciton and splits into upper and lower polariton. In a typical dispersion relation, the UPB begins at the longitudinal eigenenergy of exciton ($\hbar\omega_L$) for $\boldsymbol{k} = 0$ and bends upward with increasing $\boldsymbol{k}$, whereas the LPB starts from $\hbar\omega = 0$ and $\boldsymbol{k} = 0$ and adjusts to transverse eigenenergy of exciton ($\hbar\omega_T$) at high $\boldsymbol{k}$ states above the bottleneck region[25]. Around this bottleneck region, the splitting between UPB and LPB has a minimum value, which is proportional to the L–T splitting ($\Delta_{LT} = \hbar\omega_L - \hbar\omega_T$). In AlN, Δ_{LT} can reach up to 7.3 meV with the oscillator strength ($F = 1.14 \times 10^{-2}$). This value is much larger than that of GaAs and seven times larger than the splitting in GaN, revealing an intrinsically strong light-matter coupling strength in AlN semiconductor.

Furthermore, for wurtzite AlN, the valence band at the Γ point of the Brillouin zone is divided into three bands by spin–orbital and crystal–field splitting. Given a negative crystal–field splitting, the transition of A–exciton is $\Gamma7 \times \Gamma7$, which can be decomposed into $\Gamma1 + \Gamma2 + \Gamma5$. Only the Γ1 and Γ5 symmetries are dipole allowed for the polarization of light parallel and perpendicular to the c axis, respectively[26]. However, for A–exciton in AlN, the oscillator is almost completely excited by light in $\boldsymbol{E}\|c$ and $\boldsymbol{k}\perp c$ (π–polarization). Related light emission is strongly polarized for $\boldsymbol{E}\|c$ (polarization ratio P = 0.995) and has a maximum light intensity perpendicular to the c–axis[27]. For GaN, P is estimated as 0.5[27]. Similarly, in ZnO, the component of $\boldsymbol{E}\|c$ polarization emission is comparable with the $\boldsymbol{E}\perp c$ component[7]. Considering the high refractive index of AlN (n = 2.8 at 6.0 eV) and the atomically flat surface, significant amount of light will be confined in epitaxial film by total internal reflection. Therefore, the purely π–polarized light emission implies that majority of the confined light will couple with A–exciton, leading to a higher coupling efficiency than in GaN or ZnO. If the AlN semiconductor has microcavity structure, then the coupling strength will be expected to reach a significantly large value. Here we suggest a whispering gallery resonator[7] different from the conventional planar microcavity in the AlN (0001) orientation because of the high refractive index and strong π–polarization emission of AlN semiconductor.

For the exciton–polariton condensation, the LO phonon–assisted process is an efficient way of accelerating the polariton relaxation and reducing the stimulation threshold in strongly coupled microcavities[28]. Due to the strong ionic nature and low symmetry of the wurtzite structure of group III–nitrides, the Frohlich interaction with LO phonon becomes the dominant interaction[29,30] and AlN owns the largest LO phonon energy of 110 meV among III–nitrides. Therefore, only the LO phonon–assisted emission is observed in our spectra. Considering the exciton–like nature around or above the bottleneck region, polariton–LO phonon coupling can be expressed by the Huang–Rhys factor[31]. At all temperatures, the contribution of the pth LO phonon replica is related to zero phonon line, which is expressed by

$$\frac{F_p}{F_0} = \left(\frac{n+1}{n}\right)^{p+2} \frac{I_p\left[2S\sqrt{n(n+1)}\right]}{I_0\left[2S\sqrt{n(n+1)}\right]}$$
$$n = \frac{1}{e^{\hbar\omega_0/kT} - 1}, \qquad (2)$$

where p represents the number of LO phonon involved, n is the thermal average of the vibrational quantum number, $\hbar\omega_0$ is the LO phonon energy, I_p means the modified Bessel function with imaginary argument of order p, and S is the Huang–Rhys factor, which provides quantitative description of exciton–phonon coupling strength. By analyzing the CL and PL intensities of the pth replica, the obtained S factors of LPB_A are lower than 0.08. The value of S indicates strong exciton–phonon interaction in AlN compared with in GaN (lower than 0.01)[29], which provides efficient relaxation that bypasses the slow–acoustic–phonon thermalization process and suppresses the polariton bottleneck effect.

The abovementioned analysis denotes that the AlN semiconductor is a new candidate for the realization of polariton coherence at high temperature and even at room temperature. (1) By improving the crystal quality and purity of epitaxy films, the formation of exciton–polariton can be observed in AlN semiconductor. (2) Given their large binding energy (about 55 meV of free A–exciton), the exciton–polariton is stable at room temperature, which is the most important factor for high–temperature polariton coherence.

(3) Strong oscillator strength and purely polarized light emission obtain a record Rabi splitting of 44 meV in the thin film, which is expected to be enlarged in microcavities. (4) With an energy of 110 meV, the LO phonon in AlN can rapidly cool down the polariton and can suppress the bottleneck effect in polariton relaxation. These properties found in the AlN semiconductor will help achieve high operation temperature and low critical excited density for exciton–polariton condensation.

Discussion

The AlN film grown by MOVPE has been investigated in this work. AFM and optical measurement results show that the AlN film has high crystal quality and purity. At low temperature region, both the temperature–dependent luminescence spectra and the calculated result show an anticrossing behavior. We identified that this behavior originated from the formation of exciton–polariton because of intrinsically strong oscillator strength and purely polarized emission in AlN semiconductor. The LO–phonon–assisted transition is considered the strongest polariton–phonon interaction that plays the most important role in polariton relaxation. We demonstrated that the factors observed in the AlN semiconductor system are mostly adapted for the further improvement of polariton coherence, for the continuation of studies on polariton physics, and for the development of novel polariton devices, such as optical spin Hall effect[32], branch entanglement[33], quantum degeneracy[34], polariton superfluid transition[35], and ultrafast parametric amplifiers[36].

Methods

Fabrication. The sample investigated was a *c* (0001)–orientated undoped AlN epitaxial film grown by low–pressure MOVPE (Thomas Swan 3 × 2 in. close–coupled shower head) on the *c*–face sapphire by using trimethylaluminum (TMAl) and ammonia (NH_3) as precursors, and H_2/N_2 as the carrier gas. Low–temperature AlN buffer was first deposited in a V/III ratio of 2400 at 800°C, followed by high–temperature AlN layer at 1080°C with a V/III ratio of 400.

Measurements. The morphology of the epilayer was investigated by AFM (SPA400, Seiko Instruments Inc.). CL spectra were obtained by using an electron gun (Orsay Physics "Eclipse" FEB Column), which was installed in an ultrahigh vacuum chamber (manufactured by RHK technology). Sample can be excited at various temperatures inside a cooling cryostat. The electron beam was operated at 15 kV with current density of 7×10^{-2} A·cm^{-2}. The emitted light was dispersed by a 320 mm focal–length monochromator (Horiba Jobin Yvon iHR320) equipped with 1200 groves/mm gratings with a spectral resolution of 0.06 nm. A cooled photomultiplier tube was mounted to the monochromator. PL measurements were performed via mode–locked frequency quadrupled Ti–sapphire laser (177 nm) with power of 0.3 mW as an excitation source. The pulse width and repetition rate were 100 fs and 76 MHz, respectively. The incidence and collection angles of light on the sample were 90° and 45°, respectively.

1. Kasprzak, J. *et al*. Bose-Einstein condensation of exciton polaritons. *Nature* **443**, 409–414 (2006).
2. Balili, R., Hartwell, V., Snoke, D., Pfeiffer, L. & West, K. Bose-einstein condensation of microcavity polaritons in a trap. *Science* **316**, 1007–1010 (2007).
3. Christopoulos, S. *et al*. Room-temperature polariton lasing in semiconductor microcavities. *Phys. Rev. Lett.* **98**, 126405 (2007).
4. Tsintzos, S. I., Pelekanos, N. T., Konstantinidis, G., Hatzopoulos, Z. & Savvidis, P. G. A GaAs polariton light-emitting diode operating near room temperature. *Nature* **453**, 372–375 (2008).
5. Savvidis, P. G. *et al*. Angle-resonant stimulated polariton amplifier. *Phys. Rev. Lett.* **84**, 1547–1550 (2000).
6. Tartakovskii, A. I. *et al*. Relaxation bottleneck and its suppression in semiconductor microcavities. *Phys. Rev. B* **62**, R2283–R2286 (2000).
7. Sun, L. X. *et al*. Direct observation of whispering gallery mode polaritons and their dispersion in a ZnO tapered microcavity. *Phys. Rev. Lett.* **100**, 156403 (2008).
8. Zamfirescu, M., Kavokin, A., Gil, B., Malpuech, G. & Kaliteevski, M. ZnO as a material mostly adapted for the realization of room-temperature polariton lasers. *Phys. Rev. B* **65**, 161205(R) (2002).
9. Malpuech, G. *et al*. Room-temperature polariton lasers based on GaN microcavities. *Appl. Phys. Lett.* **81**, 412–414 (2002).
10. Faure, S., Guillet, T., Lefebvre, P., Bretagnon, T. & Gil, B. Comparison of strong coupling regimes in bulk GaAs, GaN, and ZnO semiconductor microcavities. *Phys. Rev. B* **78**, 235323 (2008).
11. Feneberg, M., Leute, R. A. R., Neuschl, B., Thonke, K. & Bickermann, M. High-excitation and high-resolution photoluminescence spectra of bulk AlN. *Phys. Rev. B* **82**, 75208 (2010).
12. Murotani, H. *et al*. Temperature dependence of excitonic transitions in a-plane AlN epitaxial layers. *J. Appl. Phys.* **105**, 83533 (2009).
13. Taniyasu, Y., Kasu, M. & Makimoto, T. An aluminium nitride light-emitting diode with a wavelength of 210 nanometres. *Nature* **441**, 325–328 (2006).
14. Taniyasu, Y. & Kasu, M. Origin of exciton emissions from an AlN p-n junction light-emitting diode. *Appl. Phys. Lett.* **98**, 131910 (2011).
15. Onuma, T. *et al*. Free and bound exciton fine structures in AlN epilayers grown by low-pressure metalorganic vapor phase epitaxy. *J. Appl. Phys.* **105**, 23529 (2009).
16. Onuma, T. *et al*. Exciton spectra of an AlN epitaxial film on (0001) sapphire substrate grown by low-pressure metalorganic vapor phase epitaxy. *Appl. Phys. Lett.* **81**, 652–654 (2002).
17. Silveira, E. *et al*. Near-bandedge cathodoluminescence of an AlN homoepitaxial film. *Appl. Phys. Lett.* **84**, 3501–3503 (2004).
18. Yamada, Y. *et al*. Photoluminescence from highly excited AlN epitaxial layers. *Appl. Phys. Lett.* **92**, 131912 (2008).
19. Leute, R. A. R. *et al*. Photoluminescence of highly excited AlN: Biexcitons and exciton-exciton scattering. *Appl. Phys. Lett.* **95**, 31903 (2009).
20. Chen, L. *et al*. Band-edge exciton states in AlN single crystals and epitaxial layers. *Appl. Phys. Lett.* **85**, 4334–4336 (2004).
21. Paskov, P. P., Paskova, T., Holtz, P. O. & Monemar, B. Polarized photoluminescence of exciton-polaritons in free-standing GaN. *Phys. Stat. Sol. (a)* **201**, 678–685 (2004).
22. Guo, Q., Nishio, M., Ogawa, H. & Yoshida, A. Temperature effect on the electronic structure of AlN. *Phys. Rev. B* **64**, 113105 (2001).
23. Strzalkowski, I., Joshi, S. & Crowell, C. R. Dielectric constant and its temperature dependence for GaAs, CdTe, and ZnSe. *Appl. Phys. Lett.* **28**, 350–352 (1976).
24. Toropov, A. A. *et al*. Temperature-dependent exciton polariton photoluminescence in ZnO films. *Phys. Rev. B* **69**, 165205 (2004).
25. Klingshirn, C. F. *Semiconductor Optics* (Springer, Berlin, 2007).
26. Laskowski, R. & Christensen, N. E. Ab initio calculations of excitons in AlN and Elliott's model. *Phys. Rev. B* **74**, 75203 (2006).
27. Taniyasu, Y., Kasu, M. & Makimoto, T. Radiation and polarization properties of free-exciton emission from AlN (0001) surface. *Appl. Phys. Lett.* **90**, 261911 (2007).
28. Pau, S. *et al*. LO-phonon-enhanced microcavity polariton emission. *Phys. Rev. B* **55**, R1942–R1945 (1997).
29. Zhang, X. B., Taliercio, T., Kolliakos, S. & Lefebvre, P. Influence of electron-phonon interaction on the optical properties of III nitride semiconductors. *J. Physics-Condensed Matter* **13**, 7053–7074 (2001).
30. Lee, B. C., Kim, K. W., Dutta, M. & Stroscio, M. A. Electron–optical-phonon scattering in wurtzite crystals. *Phys. Rev. B* **56**, 997–1000 (1997).
31. Huang, K. & Rhys, A. Theory of light absorption and non-radiative transitions in F-centres. *Proc. R. Soc. London. Ser. A. Math. Phys. Sci.* **204**, 406–423 (1950).
32. Kavokin, A., Malpuech, G. & Glazov, M. Optical spin Hall effect. *Phys. Rev. Lett.* **95**, 136601 (2005).
33. Xie, W. *et al*. Room-temperature polariton parametric scattering driven by a one-dimensional polariton condensate. *Phys. Rev. Lett.* **108**, 166401 (2012).
34. Deng, H. *et al*. Quantum degenerate exciton-polaritons in thermal equilibrium. *Phys. Rev. Lett.* **97**, 146402 (2006).
35. Amo, A. *et al*. Superfluidity of polaritons in semiconductor microcavities. *Nat. Phys.* **5**, 805–810 (2009).
36. Saba, M. *et al*. High-temperature ultrafast polariton parametric amplification in semiconductor microcavities. *Nature* **414**, 731–735 (2001).

Acknowledgments

We would like to thank Li Chen and Xiaolong Zhuo for their experimental assistance. This work was supported by National Key Basic Research Program of China (973 Program No. 2012CB619300, 2011CB925600) and National Natural Science Foundation of China (No. 61227009, No. 91321102).

Author contributions

N.G., H.Y.C. and S.P.L. fabricated the sample. K.Y.L., W.Y.W., W.H.Y. and W.L. carried out the measurements, and K.Y.L. performed the numerical simulations. K.Y.L., W.Y.W., Z.H.C., H.L., P.J. and J.Y.K. analyzed the results. K.Y.L. and J.Y.K. wrote the manuscript. H.L. and J.Y.K. supervised the study. All the authors reviewed the manuscript.

Additional information

Competing financial interests: The authors declare no competing financial interests.

How to cite this article: Li, K.Y. *et al*. Vacuum Rabi Splitting of Exciton–Polariton Emission in an AlN Film. *Sci. Rep.* **3**, 3551; DOI:10.1038/srep03551 (2013).